Surface Science 292 (1993) 267–275
North-Holland

surface science

Molecular modeling of ethylene decomposition on platinum surfaces

P.D. Ditlevsen, M.A. Van Hove and G.A. Somorjai

Materials Sciences Division, Lawrence Berkeley Laboratory and Department of Chemistry, University of California, Berkeley, CA 94720, USA

Received 21 May 1992; accepted for publication 31 March 1993

We examine the process of dehydrogenating ethylene over the (111) and (100) platinum single crystal surfaces from a modeling point of view. In order to establish the reaction pathways and the important reaction coordinates, the stability and concentration of intermediate surface species must be known. We use a simple semi-empirical tight-binding scheme, based on the extended Hückel theory. In order to model the potential energy hyper-surface (PES) on which the energy minima are found, we use a pair-potential model to describe the repulsion, similar to the ASED-MO and other methods. We fit the parameters of the pair-potential to the vibrational properties of simple molecules and adsorbates. The energy is minimized with respect to all the coordinates of the hydrocarbons on the surface using the conjugate gradient method. On the Pt(111) surface ethylidyne (CCH_3) is the most stable species. On the unreconstructed Pt(100) surface we find that the situation is different: ethylidyne is very unstable, in agreement with a recent HREELS study. This is because there are no threefold coordinated sites on the (100) surface and the repulsive part of the potential dominates in the fourfold adsorption site. The reaction barriers have been estimated by smoothly transforming the coordinates of the reactants into those of the products, while the energy of the transition state was simultaneously minimized with respect to the relevant coordinates. In this way we believe that the barriers have been determined with sufficient accuracy within the model. The general trend is that the barriers for hydrogenation–dehydrogenation from the adsorbate to the surface are considerably lower than the barriers for hydrogen transfer within the adsorbate (isomerization), which in turn is lower than that of a concerted reaction, like $CHCH + 2H \rightarrow CH_2CH_2$. From this we can determine the decomposition pathway for the ethylene to ethylidyne transition, in agreement with the findings of the ASED-MO method by Anderson.

1. Introduction

The catalytic transformation of hydrocarbons over metal catalysts is of dominating industrial interest. Even though the hydrogenation and dehydrogenation of ethylene over platinum catalysts has been investigated in detail since the 1920s and by surface science studies during the last decade [1–3], there is still no consensus about the detailed reaction pathways of the processes.

In recent years the hydrogenation process has been studied under various catalytic conditions. The ethylene hydrogenation chemistry over single crystal surfaces is similar over Pt(111) and Rh(111) [4], although these surfaces do have significantly different chemistry in general [5]. Likewise the structure dependence has been studied by performing the catalytic reaction over various crystallographic faces of the same metal [6]. These studies indicate that the hydrogenation process is, by and large, structure insensitive. The same is not necessarily true for the decomposition process. In this respect Pt(111) is by far the most investigated surface. Various surface sensitive techniques show that ethylidyne is present, in the 300–400 K range, on the (111) surface during the hydrogenation reaction [7,8]. Laser induced desorption (LID) studies [9] show that di-σ bonded ethylene decomposes to form ethylidyne. High-resolution electron energy loss spectroscopy (HREELS) studies [10] and ^{14}C-isotope studies [11] show that ethylidyne is a dead end, and not an active intermediate, in the hydrogenation of ethylene to ethane. Temperature desorption spectroscopy

(TDS) and near-edge X-ray absorption fine structure (NEXAFS) studies [12] indicate that the first H–C bond cleavage is the rate limiting step for ethylene decomposition to ethylidyne. Low-energy electron diffraction (LEED) [8] studies show that ethylene and ethylidyne form ordered overlayers on the (111) surface. An overview of the experimental studies of the Pt(111) surface can be found in ref. [13].

The clean Pt(100) surface reconstructs in a hexagonal-like pattern. Time-dependent adsorption experiments with CO have shown that a low coverage of adsorbates lifts this reconstruction [14], so that in the working catalytic conditions the (100) face will be the unreconstructed one. In a recent HREELS study [15] ethylidyne could not be found on the (100) face; this was attributed to the fact that there are no threefold sites on the unreconstructed (100) face.

The basic mechanism for the hydrogenation and dehydrogenation, namely sequential addition or subtraction of surface bound hydrogen atoms to or from the adsorbed hydrocarbon intermediates was proposed already in 1934 by Horiuti and Polanyi [16]. This mechanism seems to be the dominant pathway in the dehydrogenation and creation of intermediate surface species.

In a recent experiment by Yoshitake and Iwasawa [17], the effect of Na_2O promotion on the hydrogenation of ethylene over platinum was studied. These studies suggested that the hydrogenation of di-σ ethylene takes place at the bare metal sites while the dominating chemistry near the Na_2O promoter was via π bonded ethylene that is not present at working temperatures on the unpromoted surface. This indicates that the important hydrogenation chemistry on the unpromoted surface does indeed take place over the flat crystal faces, in contrast to proposals [18] that the chemistry takes place at defects or other special sites. However, the surface structure independence of the hydrogenation process and the presence of strongly bound intermediates during the catalytic reaction indicates that the metal surface only plays a secondary role and that the hydrogenation takes place via the adsorbed hydrocarbon layer. This mechanism was proposed by Thomson and Webb [19] in 1976, but has not yet been verified experimentally or by molecular modeling.

In this paper we address the question of characterizing the energetics, geometry, and decomposition pathways for the adsorbed hydrocarbons, present under catalytic conditions, formed by ethylene adsorption. This information is important for understanding the full catalytic process, but it is difficult to obtain experimentally since it is not readily accessible to analytic investigation, like TDS, simply because the intermediates are persistent on the surface and might transform into one another below the desorption temperature. By spectroscopic means only the very stable di-σ bonded ethylene and ethylidyne have been seen with certainty on the surface.

We do not consider the hydrogenolysis products, obtained by breaking the C–C bond. This is, on platinum, more difficult than breaking the C–H bonds and takes place at temperatures above 400–500 K.

The adsorption sites and energies of the surface intermediates and the reaction pathways are determined by minimizing the energy of the system. First-principles calculations are feasible with the increasing computing power available for calculating the energetics of complex systems with many atoms. However, for the 5d metals the relativistic motion of the electronic cores is important and these systems have not been studied, to our knowledge, by accurate first-principles calculations.

The energetics of hydrocarbon fragments on metal surfaces have been previously studied by extended Hückel theory [20–24]. The extended Hückel theory cannot predict the adsorption geometries because the repulsive part of the interatomic interactions is not adequately represented. This means that the search for the minimum energy configuration must be constrained, or the geometry assumed. One could expect that with a more realistic potential energy hypersurface (PES) more favorable configurations could be found.

We use a simple tight binding scheme based on the extended Hückel theory to model the PES. In order to describe the interatomic repulsion at small distances and thus determine bond lengths,

repulsive pair-potentials are added to the molecular orbital energy; descriptions of this approach can be found in refs. [25,26].

2. The energy calculation

The energetics of the intermediate surface species are determined by local minima of the potential energy hyper-surface (PES), which is the potential energy of the system as a function of the coordinates of the atoms.

The energies involved in relaxations on clean and covered close-packed surfaces that do not reconstruct, such as the Pt(111) surface, are of the order of phonon energies [27] which are usually unimportant in the chemical reactions where bond breaking involves much higher energies. Therefore, in this work, we consider the metal surface to be static, i.e. unrelaxed, assuming the changes of the substrate to be of minor importance. Furthermore, the extended Hückel theory can be viewed as a crude, non-self-consistent approximation, in comparison with the Hartree–Fock theory, which in turn sometimes provides grossly inaccurate results. With these limitations in mind we believe that the extended Hückel theory does provide useful information on the energetics of the hydrocarbon species adsorbed on the surface, particularly for illuminating trends. At present the examination of these systems is not feasible with more accurate methods.

We have used the slightly modified weighted formula for the extended Hückel matrix elements [28]. The extended Hückel and the Slater orbital parameters are the ones found in the literature [20] and are listed in table 1. The interatomic repulsion can be modeled by treating the extended Hückel coupling factor K as a distance dependent function [29]. A very good discussion of the extended Hückel theory and the coupling factor can be found in ref. [30].

We use a simple empirical model to describe the repulsive potential [26]. This repulsive part of the binding energy is electrostatic in nature [25] and can be approximated by pair potentials, so that the atomization energy becomes

$$E = E_{\mathrm{EHT}} + \tfrac{1}{2} \sum_{I \neq J} V_{IJ}. \tag{1}$$

The pair potentials are modeled by exponentials of the form

$$V_{IJ}(r) = \mathrm{e}^{a_{IJ} - r/b_{IJ}}. \tag{2}$$

The parameters, a_{IJ} and b_{IJ}, for the pairwise repulsions are fitted to the bond lengths and the interatomic force constants deduced from the vibrational spectra of the hydrogen, methane and acetylene molecules. Acetylene was chosen for fitting the C–C bond parameters because the extended Hückel theory itself gives too small a value for the stretching frequencies of the single (ethane) and double (ethylene) bonds. This cannot be correctly fitted using the simple form (2) for the correction. The C–C bond parameters are thus fitted to a bonding situation different from the one which is to be investigated, and we are not considering C–C bondbreaking. The interatomic force constants of the hydrocarbons are taken from ref. [31]. The platinum–hydrogen parameters are fitted to the measured values of the bond length [32] and the asymmetric vibration [33] of atomic adsorbed H on Pt(111). The platinum–carbon parameters are fitted to the measured bond length [8] and perpendicular vibration [34] of ethylidyne on Pt(111). The parameters are shown in table 2.

The atomic orbitals included in the extended Hückel calculation for the platinum are the 5d, 6s, and 6p's. The inclusion of the 6p's is important since the s and d orbitals have even symmetry and the atom can only polarize through the odd-symmetry p orbitals.

Table 1
Parameters used in the extended Hückel calculations

Atom	Orbital	H_{ii} (eV)	ζ_1	ζ_2	C_1 [a]	C_2 [a]
Pt	5d	−12.50	6.013	2.696	0.6334	0.5513
	6s	−10.00	2.554			
	6p	−5.40	2.554			
C	2s	−21.40	1.625			
	2p	−11.40	1.625			
H	1s	−13.60	1.300			

[a] Coefficients used in the double-ζ expansion of the d orbitals.

Table 2
Repulsive pair-potential parameters a and b; the experimental bond lengths, r_0, and force constants, K, are for hydrogen, methane and acetylene molecules, and for atomic hydrogen and ethylidyne on Pt(111)

	r_0 (Å)	K (eV Å^{-2}) [mdyn Å^{-1}]	a	b (Å)
H–H	0.75	24.4 [3.91]	6.2	0.11
H–C	1.10	34.2 [5.48]	20.0	0.05
C–C	1.20	102.5 [16.42]	23.3	0.05
H–Pt	1.70	5.7 [0.91]	7.5	0.17
C–Pt	2.00	19.0 [3.04]	12.5	0.15

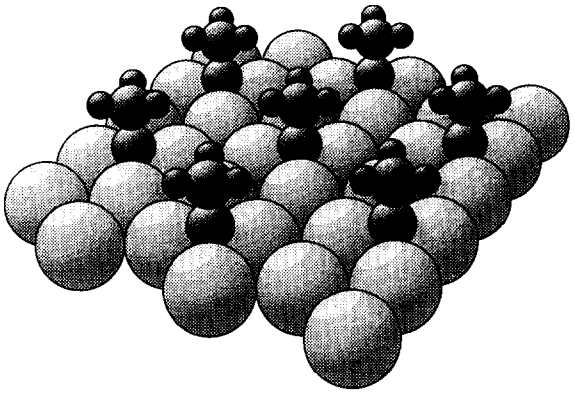

Fig. 1. Ethylidyne on Pt(111). The geometry is optimized with respect to the coordinates of the hydrocarbon. The unit cell is the (2×2) cell containing 1 hydrocarbon species.

3. Adsorption energies

The energy calculations are performed with periodic boundary conditions in two dimensions. The unit cell is (2 × 2), containing one hydrocarbon molecule. The metal is found to be sufficiently well represented by a 3 layer slab [23], containing 12 metal atoms in the unit cell. This structure corresponds to the periodicity of the ordered overlayers of ethylene and ethylidyne observed experimentally on Pt(111) at 1/4 monolayer coverage. We assume the geometry of the (100) surface to be the unreconstructed one, which is the case in catalytic conditions where the adsorbates lift the reconstruction of the clean surface. The geometry is illustrated in fig. 1 in the case of ethylidyne on Pt(111).

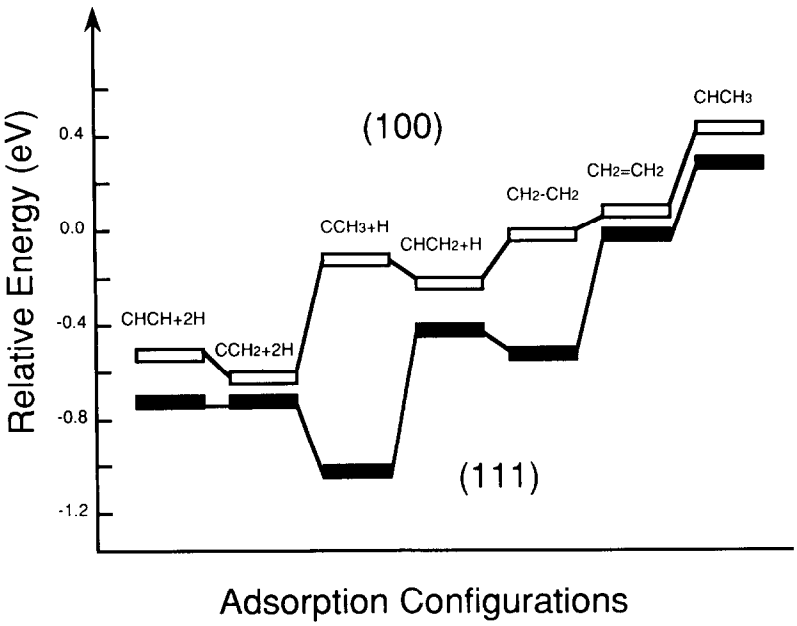

Fig. 2. Calculated energy diagram of the surface species on Pt(111) and Pt(100). The two configurations CH_2–CH_2 and CH_2=CH_2 are di-σ and π bonding types, respectively. See table 4 for details of the adsorption geometries and fig. 3 for details of the bonding configurations.

An energy minimization with respect to all the coordinates of the molecule has been performed for each of the possible hydrocarbon species on the surface. This is done by assuming reasonable starting geometries, and by the conjugate gradient method to determine the local minimum of the PES that defines a given surface species.

The results for the Pt(100) and Pt(111) surfaces are summarized in fig. 2. The adsorption energies are defined as follows: for adsorbed ethylene it is the energy of the surface–adsorbate system minus the energy of the bare surface minus the energy of the molecule; for the intermediates it is the energy of the surface–adsorbate system minus the energies of the bare surface and of the gas phase ethylene minus or plus the energy of adsorbed hydrogen atoms. So, for example: E_{ads}(ethylidyne + H) = E(surface + ethylidyne + H) − E(surface) − E(ethylene). The adsorption energy for hydrogen is defined as $E_{ads}(H) = E(\text{surface} + H) - E(\text{surface}) - \frac{1}{2}E(H_2)$.

Ethylidyne (CCH_3) is found to be the most stable species on the (111) surface; this supports the experimental finding that it is present on the surface under catalytic conditions, but it is a dead end and not an intermediate in the catalytic reaction. Vinylidene (CCH_2), vinyl ($CHCH_2$), and ethylidene ($CHCH_3$) are local minima on the potential energy hyper-surface: they are expected to be intermediates on the surface. The large relative differences in the binding energies between ethylidyne and the other intermediates explains why only ethylidyne is seen experimentally on the surface.

The adsorption energies for the different surface species on the (100) surface follow the same trend as on Pt(111) with one important exception. The ethylidyne is not very stable on the (100)

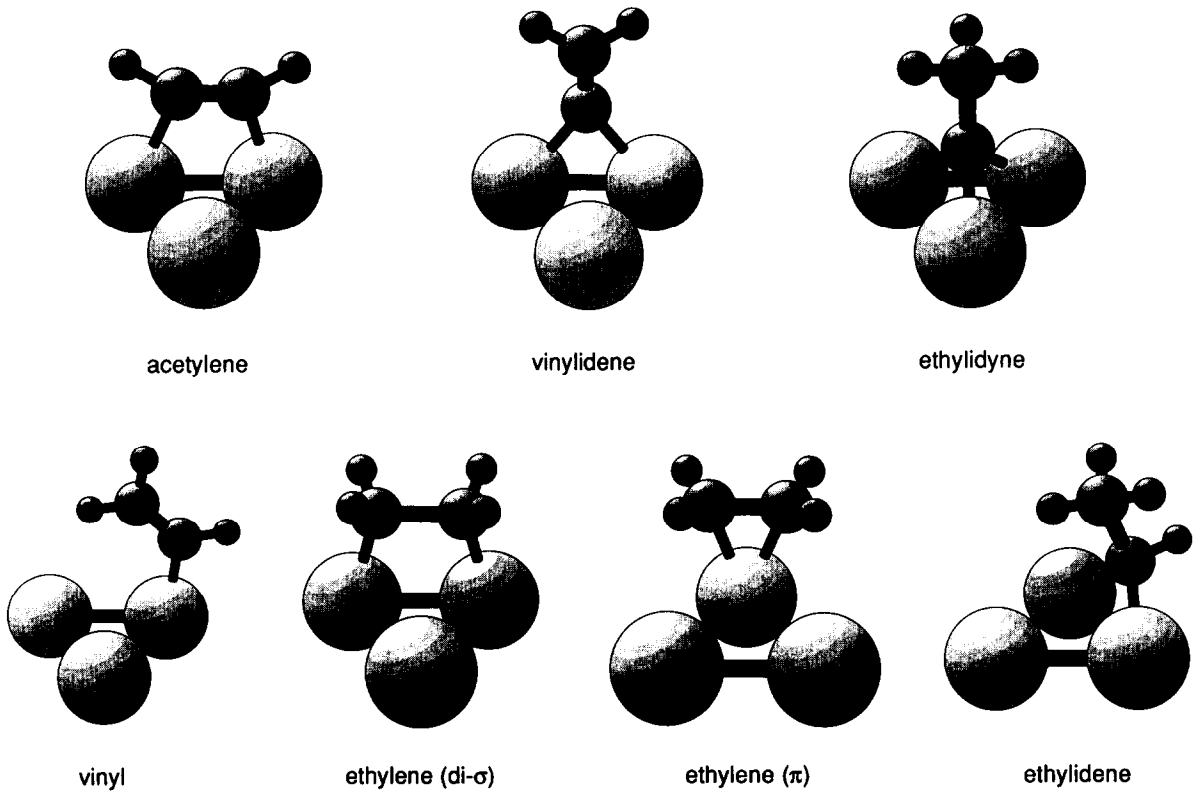

Fig. 3. The calculated adsorption geometries: the total energy of configurations are minimized with respect to all the coordinates of the hydrocarbons. The atomic radii have no physical significance.

Table 3
Calculated binding energies, in eV, of ethylidyne on Pt(111) and Pt(100)

	Attractive orbital energy	Repulsive energy	Binding energy
(111)	−2.0	1.0	−1.0
(100)	−1.9	1.8	−0.1

surface. This should be expected since the adsorption geometry on the (111) face is the tetrahedral one in the threefold site, while there are no threefold sites on the (100) face. However, this is not, as one might expect, the main reason for the difference: a MO analysis within the extended Hückel theory of the binding of ethylidyne on Rh(100) [24] shows that the fourfold site has the appropriate orbitals to bind the ethylidyne. In table 3 are shown the binding energies split into the attractive, orbital bonding term, and the repulsive, electrostatic, term. The optimum binding geometry for this model is such that the C–Pt bonds are 2.25 Å on the Pt(100) surface and 2.01 Å on the Pt(111) surface. From the table it is seen that the orbital energies for the Pt(111) and the Pt(100) surfaces are about the same; a MO analysis similar to that mentioned above for the rhodium surface also holds for the platinum surface. In the case of platinum the difference in binding energy for the two faces is dominated by the repulsive term; this is in agreement with HREELS studies in which ethylidyne could not be detected on the Pt(100) surface [15].

We did not find the ethyl radical (CH_2CH_3) to be stable on either of the two surfaces, with respect to ethylene in the gas phase and adsorbed hydrogen atoms. This means that it probably is a short-lived transition complex in the hydrogenation of ethylene to ethane.

4. Adsorption geometries

The determination from experiment of adsorption geometries for species that form ordered overlayers is today performed through LEED experiments and analysis, for example. This is a good test of the prediction of the equilibrium structures resulting from the calculation. The only LEED result for one of the species discussed here is for ethylidyne on Pt(111), for which the most recent study [8] has found a Pt–C interlayer spacing of 1.21 Å (versus 1.22 Å here) and a C–C bond length of 1.49 Å (versus 1.59 Å here): as commonly observed, EHT distances are somewhat large.

Experimentally the (111) surface is by far the most extensively studied single crystal face, so we only report the adsorption geometries of that face. Except for ethylidyne, which is not found experimentally on Pt(100), the geometries of the hydrocarbons are quite similar for the adsorption

Table 4
Optimized adsorption geometries of hydrocarbon species on Pt(111)

	Site	Bond angles (°)			Bond lengths (Å)		
		C–C tilt	C–C–H	C–H tilt	$d_{C-surf.}$	d_{C-C}	d_{C-H}
CHCH	Bridge	0	149		2.00	1.27	1.11
CCH_2	Bridge	90	124		1.68	1.29	1.11
CCH_3	Hollow	90	109		1.22	1.59	1.11
$CHCH_2$	Top [a]	42	124/122 [b]		2.04	1.34	1.11
CH_2CH_2	Bridge	0	108	30	2.00	1.70	1.09
$CH_2{=}CH_2$	Top	0	115	16	2.03	1.47	1.08
$CHCH_3$	Bridge [a]	67	109/83 [b]		1.33	1.66	1.12/1.08

All the bridge site adsorbed species are aligned parallel to the bridge. The tilt angle is defined as the angle between the bond and the surface plane, $d_{C-surf.}$ is the perpendicular distance between the surface bonded carbon and the surface plane.
[a] Approximate adsorption sites for low symmetry configurations.
[b] First angle is for the topmost C–H group, second angle is for the C–H bound to the surface.

on the (100) face. The bond angles and bond lengths are shown in table 4.

The bonding geometry of the methyl group in ethylidyne and ethylidene is tetrahedral like that of the methane molecule, as is to be expected. We do not find the triangular geometry for the acetylene previously proposed [35] to be the most stable, although the binding energy of that geometry is higher by only few tenths of an electron volt.

5. Reaction barriers

The reaction pathways of chemical reactions are the minimum energy paths on the potential energy hyper-surface (PES), leading from one local minimum representing the reactants to another local minimum representing the products. Determining the TS is in general a difficult theoretical task [36]. A high sophistication in the theoretical methods is required in order to accurately determine the energy of the transition state (TS): this is certainly not provided with the extended Hückel theory. However, with the EHT we may nevertheless expect to obtain qualitative indications. Another, practical difficulty of finding a TS is that minimization schemes will move away from the TS since it is a saddle-point. Numerical methods have been developed to determine transition states, but these methods are at present only applicable for relatively low-dimensional phase space searches. We have instead calculated the reaction barriers between different surface species by smoothly transforming one configuration into the other in such a way that the bond lengths and bond angles change monotonically and continuously. The geometry of the TS was then changed in directions perpendicular to the trajectory in phase space; if this latter search did not lower the energy of the TS significantly, it was assumed that the saddle-point was found within sufficient accuracy. In situations where different paths seemed possible the most optimal path was found.

It should be emphasized that the reaction barriers we find are not rigorously determined mathematically, however, they do, within the model, give a rigorous upper bound on the barrier heights. For this reason and due to the inaccuracy of the model we should expect to over-estimate the heights of the reaction barriers. We do, however, believe that the trends discriminating between different paths are adequately represented.

We have calculated reaction barriers between the stable surface intermediates formed after adsorption of ethylene on the Pt(111) surface. The reaction barriers are defined in fig. 4.

The difference in binding energies between A and B is given by

$$E_B - E_A = \Delta E = E_{A\to B} - E_{B\to A}. \tag{3}$$

The calculated barrier heights are listed in table 5. The ethylene listed in the table is di-σ-bonded. We find no barrier between the π-bonded and the di-σ-bonded ethylene.

The barrier for hydrogen diffusion on the surface from one hollow site across a bridge to the next hollow site was calculated to be 0.1 eV. Therefore we have assumed hydrogen always to be present in the optimal surface site for the hydrogenation processes.

Table 5
Calculated estimates of the reaction barriers $E_{A\to B}$, in eV (The reaction A → B involves (I) Isomerization, (H) Hydrogenation, (D) Dehydrogenation, or (C) Concerted mechanism)

A\B	CHCH + 2H	CCH_2 + 2H	CCH_3 + H	$CHCH_2$ + H	CH_2CH_2	$CHCH_3$
CHCH + 2H	–	3.1 (I)		1.6 (H)	3.2 (C)	
CCH_2 + 2H	3.1 (I)	–	1.8 (H)	2.1 (H)	5.5 (C)	
CCH_3 + H		2.1 (D)	–	4.6 (I)		1.3 (H)
$CHCH_2$ + H	1.3 (D)	1.8 (D)	4.0 (I)	–	1.8 (H)	
CH_2CH_2	3.0 (C)	5.3 (C)		1.9 (D)	–	4.4 (I)
$CHCH_3$			0.3 (D)		3.6 (I)	–

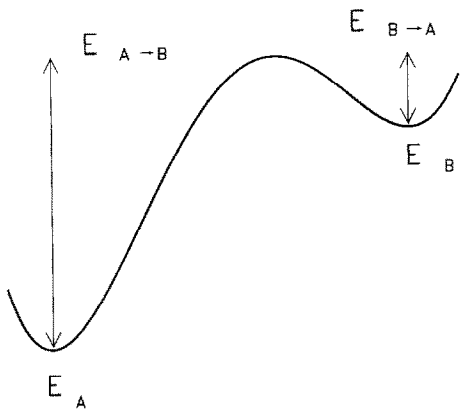

Fig. 4. The reaction barriers for the chemical reaction A → B and B → A.

From table 5 it is seen that the estimated barriers for hydrogenation/dehydrogenation processes are in the range 1–2 eV, for isomerization processes in the range 3–4 eV and for the concerted mechanisms, corresponding to two hydrogenations/dehydrogenations, in the range 3–5 eV. Although the calculated barriers are high in comparison with what would be expected from experiments, the trends in the relative heights are significant.

The concerted mechanisms like $CH_2CH_2 \rightarrow CHCH + 2H$ are not favorable; the barrier is equal to or even higher than the sum of the barriers for the stepwise reactions like $CH_2CH_2 \rightarrow CHCH_2 + H \rightarrow CHCH + 2H$. This type of reaction will furthermore be thermodynamically suppressed as is seen from entropy considerations.

For isomerization processes we find that the presence of the catalytic metal surface does not significantly lower the barriers in comparison with gas phase processes. The role of the metal surface is to mediate direct hydrogenation or dehydrogenation of adsorbed atomic hydrogen.

According to our model, the pathway from ethylene to ethylidyne will be $CH_2CH_2 \rightarrow CHCH_2 + H \rightarrow CHCH + 2H \rightarrow CCH_3 + H$, in agreement with the findings of the ASED-MO method [29]. The first barrier is slightly higher than the two subsequent ones; this is in agreement with the experimental finding [6] that the first C–H bond cleavage is the rate-limiting step. It should, however, be stressed that within this simple model we must be cautious about such small energy differences. The model in fact does conflict with recently proposed mechanisms for dehydrogenation [13] like $CH_2CH_2 \rightarrow CHCH_3 \rightarrow CCH_3 + H$ and $CH_2CH_2 \rightarrow CHCH_2 + H \rightarrow CCH_3 + H$, since they both involve isomerizations.

6. Summary

We have used a simple semi-empirical tight-binding scheme based on the extended Hückel theory to calculate the binding energies and geometries for the Pt(100) and Pt(111) surfaces and reaction barriers and decomposition pathways for hydrocarbon fragments on Pt(111).

We find that the dehydrogenation chemistry is different on the Pt(111) and the Pt(100) surfaces. Ethylidyne is the most stable adsorbate on the Pt(111) surface while it is not very stable on the Pt(100) surface. This is due to the larger carbon–metal repulsion in the fourfold site in comparison with the threefold site.

We find that the decomposition process of forming ethylidyne from adsorbed ethylene on Pt(111) takes place via the pathway: dehydrogenation of ethylene to vinyl, further dehydrogenation to vinylidene, and finally hydrogenation of vinylidene to ethylidyne.

This study of the dehydrogenation chemistry on the platinum surfaces does suggest some insight into the more important hydrogenation processes. Firstly, we find that the ethyl, which must be an intermediate or transition complex in the hydrogenation of ethylene to ethane, is not stable, in the low coverage regime, on the surfaces. Secondly, ethylidyne is very stable on the (111) surface and is not an intermediate in any catalytic reactions. This means that the surface will be covered by a layer of ethylidyne while the catalytic reaction takes place. This is not the case for the (100) surface, on which the energy differences between the different surface species are smaller than on the (111) surface. We find that the binding energies on the (100) surface are, in general,

slightly smaller than on the more close-packed (111) surface. We can conclude that the trends are the same on the two faces except the case of ethylidyne which is not stable on Pt(100). This means that the catalytic conditions under which the hydrogenation takes place are different for the two surfaces.

Acknowledgements

We are grateful for clarifying discussions with Mr. M. Quinlan and Dr. Z. Nomikou. We acknowledge useful discussions with Dr. C. Minot and his generosity in providing us with the extended Hückel codes. Support for this work was provided by the Advanced Industrial Concepts Division of the US Department of Energy under contract No. DE-AC03-76SF00098. Supercomputer time at the Florida State University Computer Center and at the University of California Los Angeles Computer Center is appreciated.

References

[1] L.L. Kesmodel, P.C. Stair, R.C. Baetzold and G.A. Somorjai, Phys. Rev. Lett. 36 (1976) 1316.
[2] M. Salmeron and G.A. Somorjai, J. Chem. Phys. 86 (1982) 341.
[3] P. Klimesch and M. Henzler, Surf. Sci. 90 (1979) 57.
[4] B.E. Bent, PhD Thesis, University of California, Berkeley, 1986.
[5] G.A. Somorjai, Chemistry in Two Dimensions: Surfaces (Cornell University Press, Ithaca, 1981).
[6] F. Zaera, PhD Thesis, University California, Berkeley, 1984.
[7] M. Quinlan, private communication.
[8] U. Starke, A. Barbieri, N. Materer, M.A. Van Hove and G.A. Somorjai, Surf. Sci. 286 (1993) 1.
[9] C.L. Pettiette-Hall, D.P. Land, R.T. Melver and J.C. Hemminger, J. Phys. Chem. 94 (1990) 1948.
[10] A.L. Backman and R.I. Masel, J. Vac. Sci. Technol. A 9 (1991) 1789.
[11] F. Zaera and G.A. Somorjai, J. Am. Chem. Soc. 106 (1984) 2288.
[12] F. Zaera, J. Phys. Chem. 94 (1990) 5090.
[13] E.A. Carter and B.E. Koel, Surf Sci. 226 (1990) 339.
[14] M. Eiswirth, P. Möller, K. Wetzl, R. Imbihl and G. Ertl, J. Chem. Phys. 90 (1989) 510.
[15] E. Yagasaki, A.L. Backman, B. Chen and R.I. Masel, J. Vac. Sci. Technol. A 8 (1990) 2616.
[16] J. Horiuti and M. Polanyi, Trans. Faraday Soc. 30 (1934) 1164.
[17] H. Yoshitake and Y. Iwasawa, J. Catal. 131 (1991) 276.
[18] R. Joyner, private communication.
[19] S.J. Thomson and G. Webb, J. Chem. Soc. Chem. Commun. (1976) 526.
[20] C. Minot, M.A. Van Hove and G.A. Somorjai, Surf. Sci. 127 (1982) 441.
[21] Ph. Sautet and J.-F. Paul, Catal. Lett. 9 (1991) 245.
[22] A. Gavezzotti and M. Simonetta, Surf. Sci. 99 (1980) 453.
[23] Y.-T. Wong and R. Hoffmann, J. Chem Soc., Faraday Trans. 86 (1990) 4090.
[24] B. Schiøtt, R. Hoffmann, M.K. Awad and A.B. Anderson, Langmuir 6 (1990) 806.
[25] A.B. Anderson, R.W. Grimes and S.Y. Hong, J. Phys. Chem. 91 (1987) 4245.
[26] L.W. Anders, R.S. Hansen and L.S. Bartell, J. Chem. Phys. 59 (1973) 5277.
[27] P.D. Ditlevsen, P. Stoltze and J.K. Nørskov, Phys. Rev. B 44 (1991) 13002.
[28] R. Hoffmann and P. Hoffmann, J. Am. Chem. Soc. 98 (1976) 598.
[29] D.B. Kang and A.B. Anderson, Surf. Sci. 155 (1985) 639.
[30] G. Calzaferri, L. Forss and I. Kamber, J. Chem. Phys. 93 (1989) 5366.
[31] L.M. Sverdlov, M.A. Kovner and E.P. Krainov, Vibrational Spectra of Polyatomic Molecules (Halsted Press, New York, 1974).
[32] K. Mortensen, F. Besenbacher, I. Stensgaard and C. Klink, Surf. Sci. 211/212 (1989) 813.
[33] A.M. Baró, H. Ibach and H.D. Bruchmann, Surf. Sci. 88 (1979) 384.
[34] H. Ibach and D.L. Mills, Electron Energy Loss Spectroscopy and Surface Vibrations (Academic Press, New York, 1982).
[35] A.B. Anderson and A.T. Hubbard, Surf. Sci. 99 (384) 1980.
[36] M. Page and J.W. McIver, J. Chem. Phys. 88 (1988) 922.